Effect of solution heat treatments on superalloys Part 1 – alloy 718

J. Andersson*[1], G. P. Sjöberg[1], L. Viskari[2] and M. C. Chaturvedi[3]

The hot ductility as measured by Gleeble testing of Alloy 718 at four different solution heat treatments (954°C/15 h, 954°C/1 h, 982°C/1 h and 1050°C/3 h+954°C/1 h) has been investigated. It is concluded that constitutional liquation of NbC assisted by δ phase takes place and deteriorates the ductility. Parameters established by analysing the ductility dependence on temperature indicate a reduced weldability of the material in the coarse grain size state (ASTM 3) while indicating an increased weldability when containing a large amount of δ phase due to a grain boundary pinning effect. The accumulation of trace elements during grain growth at the highest temperature is believed to be the cause for the observed reduced on-cooling ductility.

Keywords: Alloy 718, Hot ductility, Gleeble testing, Weldability

Introduction

All superalloys are inherently difficult to weld, due to their very high content of alloying elements which allows for the high temperature strength necessary in aircraft engines. Most difficult to weld are the precipitation hardening type of alloys. Among these, however, the sluggish γ'' hardening response of Alloy 718 significantly contributes to an exceptional good weldability[1] among these alloys. This is one of the major reasons for Alloy 718 being used for the large hot parts of aircraft engines today, which are often assembled from wrought and cast parts and joined by welding.[2]

Still, Alloy 718 is not devoid of welding problems and for many years, the susceptibility to heat affected zone liquation cracking has been a serious concern. Also the harmful effect of certain trace elements such as S, P and B is well known.[3–5]

Alloy 718 contains 5·5 wt-%Nb which provides for its very high strength by enabling the formation of the γ'' phase, but Nb also makes the alloy prone to severe segregation during solidification. In heavily segregated interdendritic areas in weld deposits and in castings, the non-equilibrium and very brittle Laves eutectic will then be present in various amounts. In these areas, the primary NbC carbides, though in equilibrium, also precipitate. Finally, Nb is an essential element in the formation of the important secondary δ phase at high temperatures.

The present investigation sheds light on the effect of metallurgical parameters on the hot ductility of Alloy 718. For this purpose, the Gleeble testing[6] and the differential scanning calometry (DSC) were used.

Of special concern was the amount of δ phase produced by different solution heat treatments, but also the effect of enlarged grains obtained through overheating.

Experimental

Material

A commercial AMS 5662, 127 mm diameter wrought bar with the chemical composition as shown in Table 1 was used for all testing in the present study.

Cylindrical test specimens, 6 mm in diameter and 120 mm in length, were excised axially, heat treated and trimmed by turning.

Heat treatments

Heat treatments at 954°C/15 h, 954°C/1 h, 982°C/1 h and 1050°C/3 h+954°C/1 h were carried out in vacuum before final machining. Forced convection cooling in argon to 500°C was used to minimise precipitation reactions during the cooling. Here, the 954°C/1 h and 982°C/1 h treatments are the lower and upper limit respectively, of the recommended solution heat treatment temperature range for Alloy 718. The 15 h heat treatment at 954°C was carried out in order to produce a large amount of δ phase. The super solvus condition at 1050°C/3 h was performed in order to dissolve all δ phase and to allow for grain growth and a coarse grain size structure.

Gleeble testing

A Gleeble 1500D system with water quench facilities was used with temperature control through percussion welded thermocouples on each test sample. Test parameters are shown in Table 2.

As proposed for Nb carrying superalloys which undergo significant liquation,[7] the on-cooling tests were initiated from the nil strength temperature of −30°C.

[1]Department of Materials Technology at Volvo Aero Corporation, 46181 Trollhättan, and Chalmers University of Technology, 41296 Gothenburg, Sweden
[2]Department of Microscopy and Microanalysis at Chalmers University of Technology, 41296 Gothenburg, Sweden
[3]Department of Mechanical and Industrial Engineering, University of Manitoba, Winnipeg, Manitoba, R3T 5V6 Canada

*Corresponding author, email joel.anderssonvolvo.com

Published by Maney on behalf of the Institute
Received 08 May 2011; accepted 10 October 2011
DOI 10.1179/1743284711Y.0000000101

In Gleeble testing, ductility is measured as the reduction of area (RA) and plotted against the temperature from which it is possible to determine certain hot ductility characteristics such as the nil ductility temperature (NDT) and the ductility recovery temperature (DRT) (at 5% RA). These data can be used to establish other parameters, such as the brittle temperature range (BTR), the ductility recovery rate (DRR) and the ratio of ductility recovery (RDR), which are considered as essential measures for estimating the susceptibility to hot cracking during welding.[8]

Microscopic examination

The fracture surface areas were measured in a stereo microscope and with analysing software.

Standard automatic metallographic preparation techniques were used with an electrolytic etching at 5 V in oxalic acid for 10 to 20 s.

Hardness was measure with the Vickers method at 10 kg load on polished surfaces.

Light optical microscopy as well as scanning electron microscopy (SEM) was used for examination of polished and etched cross-sections as for the investigating of fracture surfaces. The SEM used was a FEI Quanta 200 field emission gun SEM operated at 20 kV and mainly operated in the backscatter electron (BSEs) mode, allowing for compositional contrast. Grain size was determined by the linear intercept method.

Differential scanning calorimetry

A Netzsch STA 409 DSC thermal analysis equipment was used to examine phase transformations at low heating and cooling rates which could aid in interpreting the Gleeble results. A constant heating and cooling rate of 0·3°C s^{-1} with a 20 min dwell time at a peak temperature of 1400°C was used. The DSC samples were 5 mm diameter discs with a weight of ~50 mg. An argon gas flow of 0·17 ml s^{-1} was used for protection.

Table 1 Chemical composition of AMS 5662, wt-%

Element	Content	Element	Content
Ni	53·40	C	0·04
Cr	18·36	Mn	0·09
Fe	17·49	Si	0·05
Co	0·33	B	0·001
Mo	3·15	P	0·008
Al	0·56	S	0·0003
Ti	0·92	Cu	0·14
Nb	5·46	Ta	<0·01

Table 2 Gleeble testing parameters

Gleeble parameters	
Heating rate/°C s^{-1}	111
Cooling rate/°C s^{-1}	50
Peak temperature/°C	1195
Stroke rate/mm s^{-1}	55
Holding time at peak temperature/s	0·03
Holding time at test temperature/s	0·03
Thermocouple and diameter/mm	Chromel–alumel, 0·254

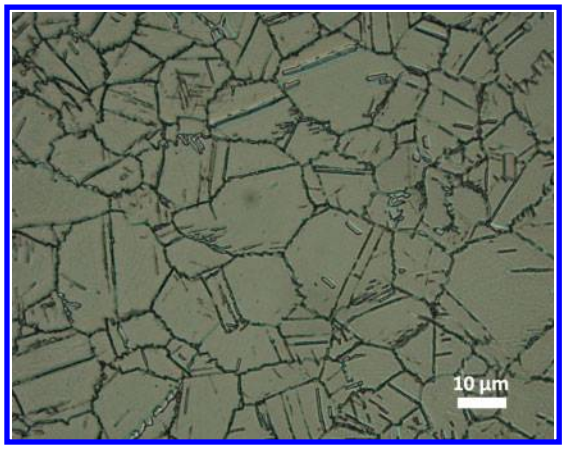

1 Microstructure of as received material: grain size ASTM 10 and hardness 260 HV

Results

Heat treatments and microstructure

The structure and the hardness of the as received material are shown in Fig. 1.

The microstructures, Vickers hardness and grain size values produced by the heat treatments at 954°C/15 h, 954°C/1 h, 982°C/1 h and 1050°C/3 h + 954°C/1 h are shown in Fig. 2. The hardness response on heat treatment were accordingly; 266 HV for the 15 h treatment at 954°C followed by 244 HV at 954°C/1 h and 254 HV at 982°C/1 h. The super solvus treatment resulted in significantly reduced hardness (161 HV).

As revealed by the micrographs in Fig. 2, the amount of δ phase depends on the solution temperatures and the dwell times. The δ phase can be found both inter- and intragranularly throughout the microstructure; however, grain and twin boundaries are favourable nucleation sites. At 954°C, which is the standard temperature used for the dissolution of the hardening γ'' phase, the amount of δ phase will increase with the dwell time, since it is a thermodynamically stable phase at that temperature. By comparison, after a 15 h dwell time significantly more δ phase is thus present than after 1 h. At 982 and 954°C, the amount of δ phase at equilibrium is estimated by JMatPro software to 5 and 8 wt-% respectively. The driving force for the precipitation is thus smaller at 982°C which is reflected in a smaller amount of δ phase after 1 h heat treatment at 982°C in comparison with the amount precipitated at 954°C. At 1050°C, however, δ phase is no longer stable and it is accordingly dissolved. The stabilising, pinning, effect of the δ phase in the grain boundaries disappears at the same time and substantial grain growth takes place as is evident from Fig. 2*d*. It should also be noted that the 1 h heat treatment at 954°C following the 1050°C/3 h exposure is evidently not long enough to precipitate any new δ phase.

Gleeble test results

In Fig. 3, RA is plotted against the testing temperature, as measured both for the on-heating and the on-cooling test cycles.

The weldability parameters BTR, DRR and RDR excised from the data plots in Fig. 3 are shown in Table 3.

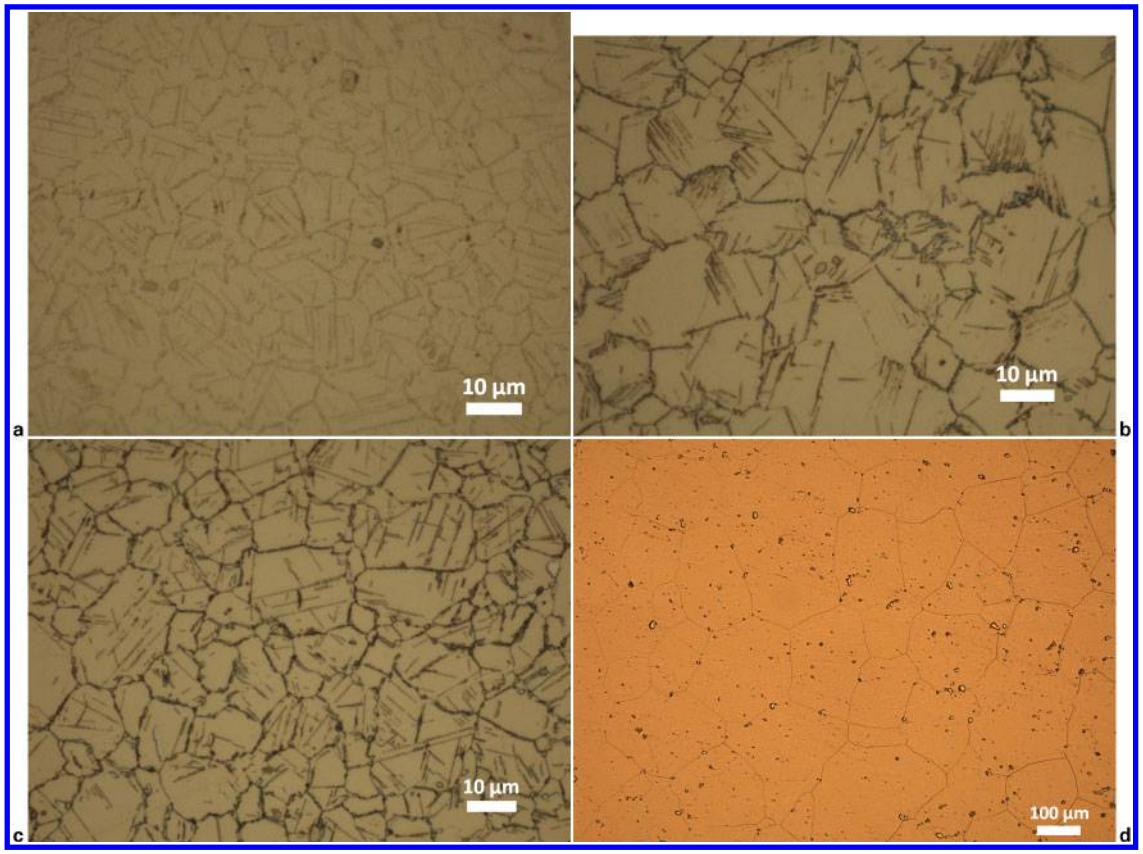

a 954°C/15 h (266 HV, ASTM 11); *b* 954°C/1 h (244 HV, ASTM 9); *c* 982°C/1 h (254 HV, ASTM 11); *d* 1050°C/3 h+954°C/1 h (161 HV, ASTM 2)

2 Microstructure, hardness and grain size achieved through different solution heat treatments

The hardness of water quenched samples from the on-heating (wqh) and from the on-cooling (wqc) cycles are presented in Figs. 4 and 5 respectively.

The 1050°C/3 h heat treatment before the testing reduced the hardness of the as received material from 260 to 160 HV and remains so when exposed to the Gleeble on-heating and quenching cycles. For the three other conditions produced at the lower solution temperatures, there is, however, a slight hardness reducing effect by the Gleeble heating cycle to the highest temperature, which is accompanied by an increase in the grain size as reflected in Table 4 and 5.

The variation of hardness of all fine grain specimens tested in the on-cooling thermal cycles is small at an average hardness level slightly above 200 HV. Compared to the on-heating hardness values, this average is

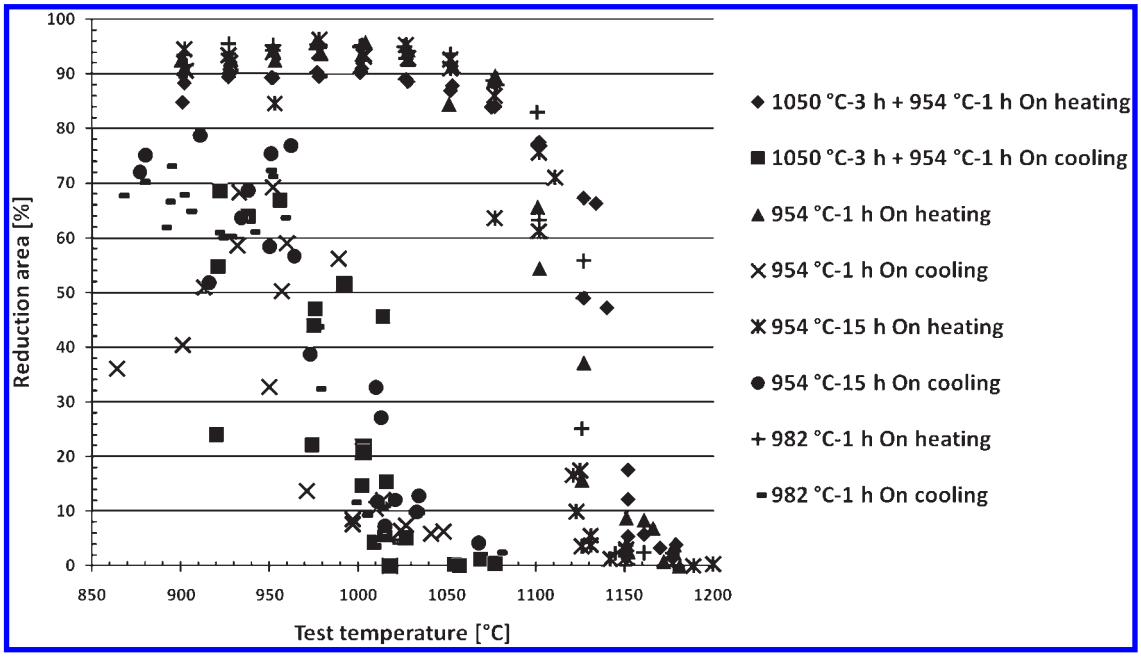

3 Hot ductility (RA) in four different heat treated conditions versus temperature in on-heating and on-cooling test cycles

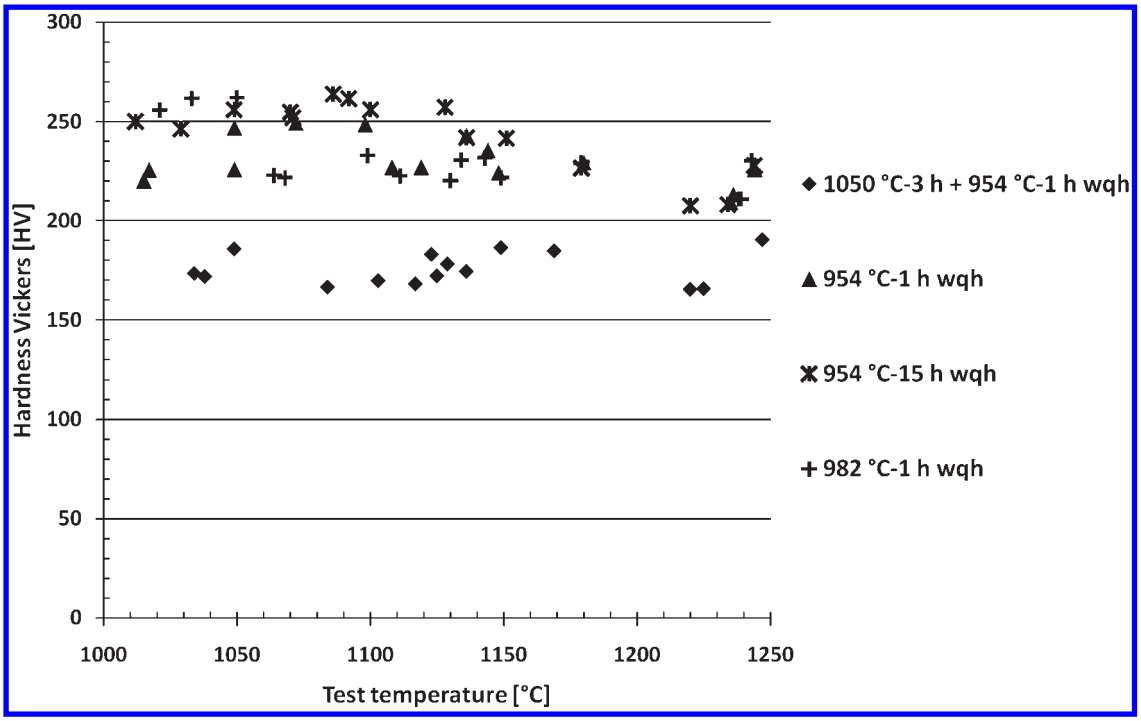

4 Hardness versus temperature for on-heating thermal cycles

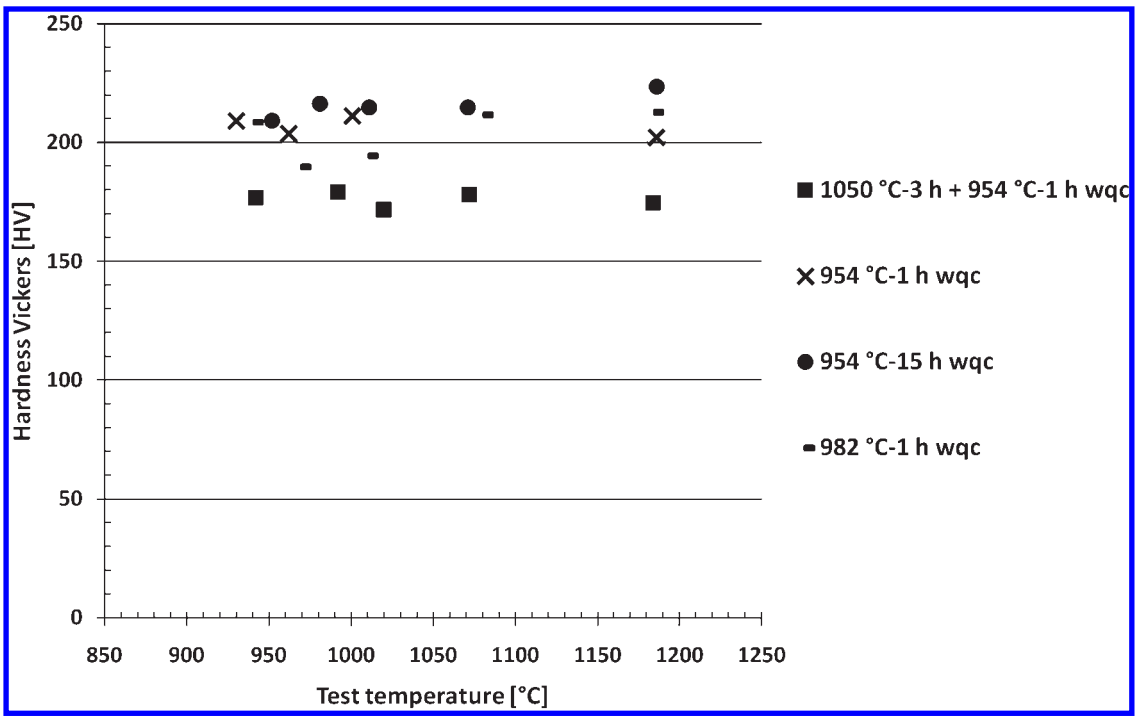

5 Hardness versus temperature for on-cooling thermal cycles

Table 3 Estimated Gleeble/weldability parameters

Hot ductility parameters	954°C/1 h	982°C/1 h	954°C/15 h	1050°C/3 h+954°C/1 h
NDT/°C	1152	1145	1131	1177
DRT/°C	1024	1020	1033	1015
BTR/°C	171	175	162	180
DRR/%	61	74	78	68
RDR/%	12	14	19	11

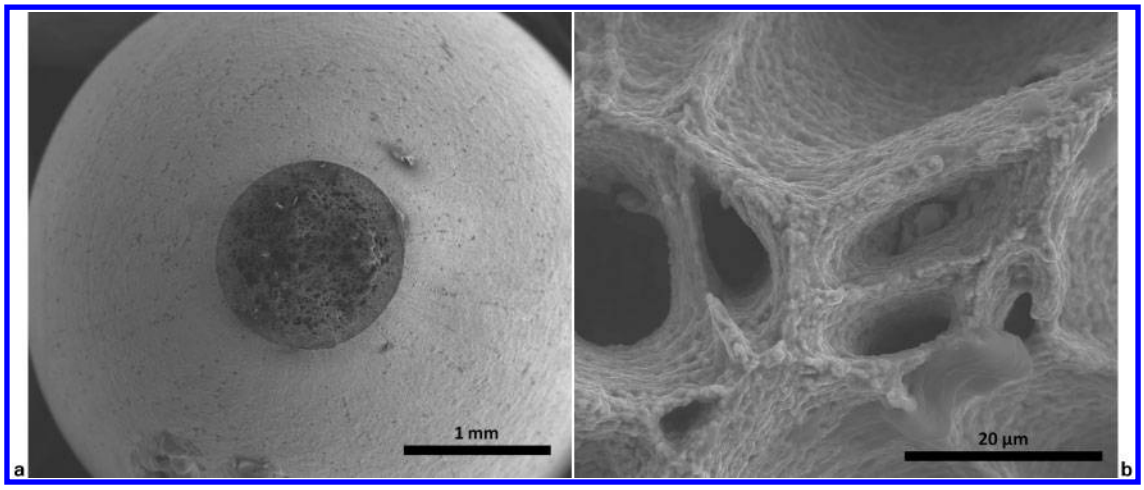

6 Typical cup and cone fracture with strong necking with fracture revealing microvoids coalescence at *a* low and *b* high magnification: 954°C/1 h heat treated material tested at 976°C

slightly lower. Furthermore, there is no reduction of the hardness for the samples tested at the higher temperature range compared with the ones tested at the lower. The hardness of the large grain material is consistently slightly less than that of the fine grain materials. All this may be explained by the grain size effect: as the on-cooling samples were all subjected to the same high temperature–time exposure cycle in the on-heating part of the cycle, this allows for certain growth and levelling out of the grain size during the few seconds spent in this temperature regime. Still, this is not comparable with the abnormal growth during the 3 h exposure for the large grain size material before testing.

Temperatures for phase transformation events, as obtained by DSC analysis, are summarised in Table 6. The temperatures are those obtained at the deviation peaks on the baseline curve.

Discussion

On-heating

The reduction of area is >80% for all four heat treatment conditions at test temperatures below 1050°C. Above 1050°C, however, the ductility is rapidly reduced to <10% at and >1150°C as evident in Fig. 3. There are small differences between the four heat treatment conditions although the material in the large grain condition exhibits a lower ductility below 1050°C. This is expected since coarse grain materials are generally known to show lower ductility than the same fine grain materials.[9,10] It is also known that if there are large amounts of δ phase present ductility will be reduced;[11] however, this effect is not seen below 1050°C.

Fracture occurs through the formation and coalescence of microvoids in a ductile manner revealed by typical cup and cone fracture surfaces as shown in Fig. 6 for material tested at 976°C and in Fig. 7 for material tested at 1050°C.

Even though the 1050°C samples are very ductile, there is a clear difference between the samples tested at 1050°C, where the rapid transition from ductile to brittle behaviour starts, and those tested at 975°C. While the cup and cone fracture behaviour still occurs at 1050°C, final fracture with microvoids coalescence does not (as evident in Fig. 7).

Above 1050°C, ductility is rapidly lost in all four material conditions. The ductility of the material in the large grain condition is lost at slightly higher temperatures (~25°C higher) in comparison with the other three material conditions as seen in Fig. 3. This may be attributed to the deleterious effect of the δ phase still present after the rapid heating (111°C s^{-1}) in the present testing. It has been shown[12] that even if the δ phase does dissolve completely above 1050°C given enough time to reach equilibrium, it may survive during rapid heating to very high temperatures where the high Nb content,

Table 5 On-cooling average grain size variation for quenched samples

Condition	Grain size/ASTM	STDEV*
954°C/1 h	8·0	0·1
982°C/1 h	7·8	1·8
954°C/15 h	9·5	0·6
1050°C/3 h+954°C/1 h	2·9	0·2

*Standard deviation of three samples

Table 4 On-heating grain size at different temperatures for quenched samples

954°C/1 h		982°C/1 h		954°C/15 h		1050°C/3 h+954°C/1 h	
Temperature /°C	Grain size/ASTM	Temperature/°C	Grain size/ASTM	Temperature/°C	Grain size/ASTM	Temperature/°C	Grain size/ASTM
1017	8	1021	10	1086	10	1034	4
1049	8	1033	10	1092	10	1038	3
1136	9	1050	10	1128	11	1049	3
1144	10	1064	9	1220	8	1220	3
1180	10	1099	9	1234	9	1225	3

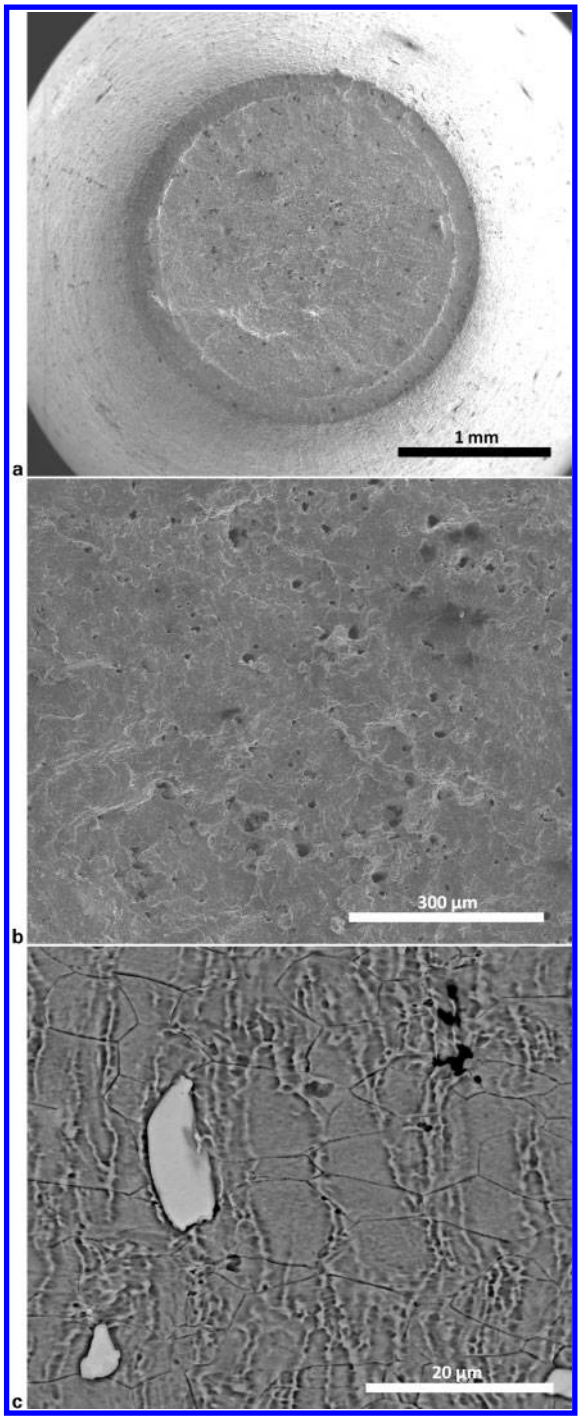

7 Images (SEM–SE) of smooth fracture surface at *a* low magnification, *b* high magnification and *c* SEM–BSE image of longitudinal section showing few microvoids and NbC from testing at 1050°C

~29·5 wt-%Nb in δ phase and 32 wt-%Nb in Laves phase,[13] will then allow for constitutional liquation in terms of the Laves eutectic reaction at ~1125°C. If this occurs, the hot ductility is completely lost by the formation of the liquid Laves eutectic at the grain boundaries.

In Fig. 8 the remains of δ phase at the grain boundaries close to the fracture surface are shown for all material conditions tested above 1125°C. At first sight the remaining traces might be interpreted as if the δ phase has been subjected to constitutional liquation and resolidified. However, there are no sharp phase boundaries between these traces and the matrix, and in addition, no traces of any Laves eutectic formation are present. It is therefore more likely that they are traces of the very fast solid state dissolution of the δ phase. Owing to the fast heating and cooling there is limited time for Nb diffusion and the concentration gradient is still very sharp which produces the relief at etching.[14] It should be noted that the SEM analysis technique used in this investigation may not be adequate to reveal the initial steps of liquation. By transmission electron microscopy technique Laves formation adjacent to δ phase has been identified.[12] It is therefore not possible to conclude if constitutional liquation of δ phase takes place or not. Although no obvious constitutional liquation of the δ phase takes place at the grain boundaries the presence of δ phase still makes the boundaries brittle as evident in Fig. 8.

In the coarse grain material, there is no δ phase to be dissolved which may explain the observed ductility shift towards higher temperature. By the same token, comparing the ductility drop of the standard heat treatment (at 954°C/1 h) to that of the material heat treated at 954°C/15 h, the latter exhibits a slight shift towards lower temperatures which may be due to the higher amount of δ phase of this material. The ductility drop in the material heat treated at 982°C/1 h is, however, shifted towards slightly higher temperatures and may again be explained by the amount of δ phase which is lower for this condition. Interestingly, the same type of temperature shifts are noted in the NDT as evident from Table 3, but these temperature shifts may be explained by the different amounts of δ phase subjected to true constitutional liquation of the δ phase above the Laves eutectic temperature.[12]

The fracture surfaces shown at a low magnification in Fig. 9 also reflect these different liquation responses where clear traces of liquation can be seen in Fig. 9*b* of the materials heat treated at 954°C for 15 h.

It should be noted that the NbC in the coarse grain material, appearing bright in Fig. 8*d*, show no obvious

Table 6 Phase transformations as measured by DSC during heating and cooling for different H/T condition

	954°C/1 h		954°C/15 h		982°C/1 h		1050°C/3 h + 954°C/1 h	
Phase reaction temperature/°C	Heating	Cooling	Heating	Cooling	Heating	Cooling	Heating	Cooling
Laves phase	ND*	1125	ND*	1117	ND*	1115	ND*	1117
MC phase	1262	1261	1286	ND*	1265	ND*	1280	ND*
Liquidus temperature	1357	1355	1350	1342	1351	1349	1350	1339

*ND: not detected.

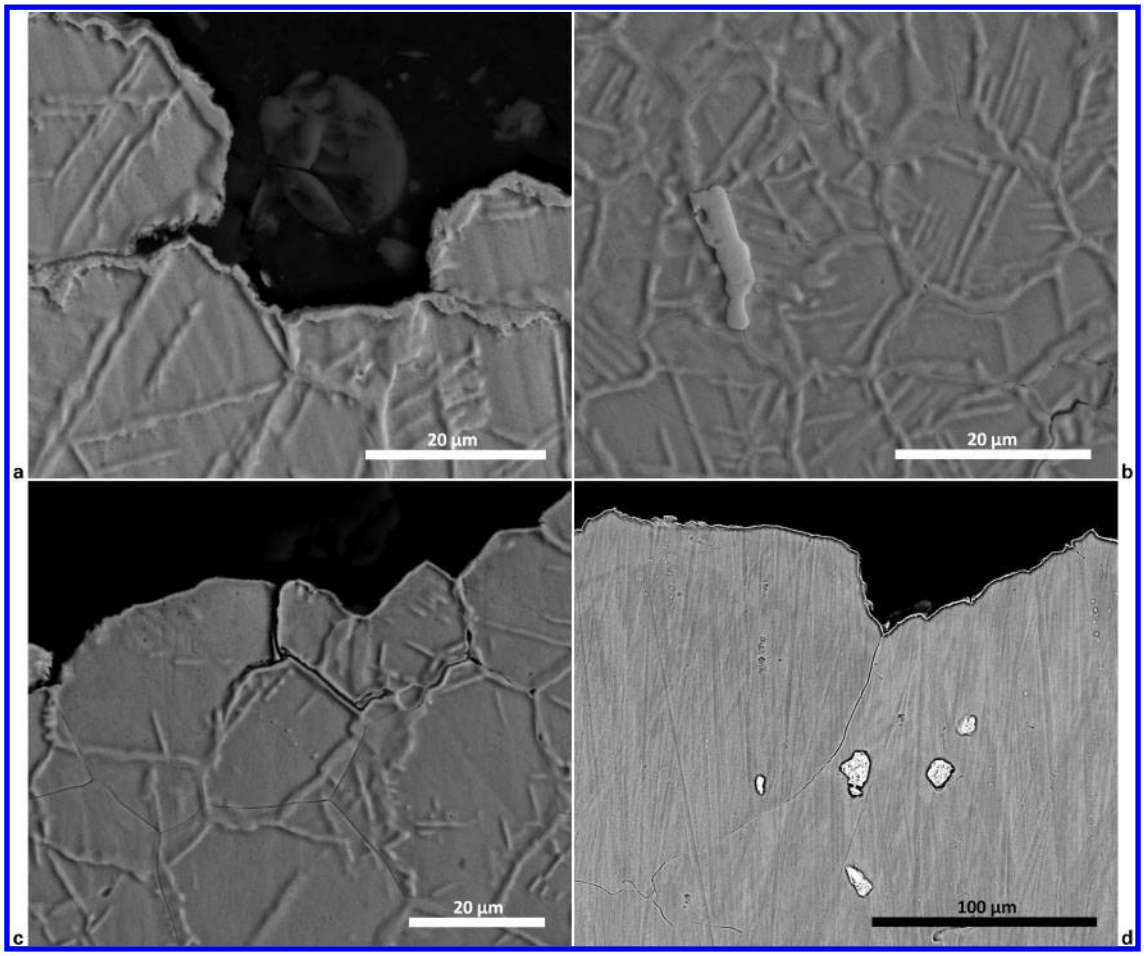

a 954°C /15 h at 1189°C; *b* 954°C/1 h at 1172°C; *c* 982°C/1 h at 1178°C; *d* 1050°C/3 h + 954°C/1 h at 1177°C

8 Images (SEM–BSE) of longitudinal cross-sections tested during on-heating thermal cycle

traces of liquation at the testing temperature of 1177°C which might be expected, since this temperature is well below the 1260°C carbide eutectic temperature (see Table 6). However, as reported in literature[15] and since the NbC and Laves phases are constituents in a three phase system, they may interact in a ternary system over a temperature range. This assumption is supported by thermodynamic theory which may encompass constitutional liquation of carbides even at such low temperatures as 1177°C.

This is also the most probable explanation for the formation of eutectics at 1077°C for the 954°C/15 h condition as shown in Fig. 10. A localised large amount of plastic work may add adiabatic heating due to the very fast deformation and thus contribute to the liquation, which may explain the fact that the formation of eutectics appears to occur preferably close to the fracture surface in the heavily necked area (60% RA). The large amount of eutectic in comparison with the limited amount of NbC available for constitutional liquation advocates that the δ phase may contribute to this process.

All testing performed on-heating above 1150°C indicates a very brittle material behaviour as evident by RA values less than 5% (Fig. 3) and the fracture surfaces (Fig. 11) for the materials heat treated at 982°C/1 h and 954°C/1 h.

It is reasonable that the more ductile behaviour when testing at the lower temperatures is also reflected in the fracture surfaces. A transition occurs from an entirely brittle grain boundary fracture to a dimpled appearance as may be seen by comparing Fig. 12 from testing at 1126°C with Fig. 11 from the testing at 1176°C for the two materials heat treated at 954°C/1 h and 982°C/1 h respectively.

By comparison, there are small differences in the on-heating ductility properties between the two heat treatment conditions 954°C/1 h and 982°C/1 h, as evident by the ductility curves in Fig. 3. This also coincides with the similar minor differences in the δ phase appearance (as shown in Fig. 2) and the NDT values in Table 3. Still, the axial sections in Fig. 13 indicate that the grain boundaries are more brittle in the 954°C/1 h condition, corresponding to a significantly lower ductility at the actual test temperature of 1126°C in the ductility transition temperature region.

On-cooling tests

From the hot ductility data in Fig. 3, it is evident that by exposing the material, in all four heat treatment states, to temperatures close to the nil strength temperature (30°C) by rapid heating, irreversible changes occur in the microstructure. These changes account for the strong negative effect on the hot ductility during the subsequent cooling. Analyses using SEM show formation of considerable amounts of eutectic constituents of two basic morphologies as shown in Fig. 14. The prerequisite for any eutectic formation is constitutional liquation of either the δ phase or the NbC during the heating up cycle.[15] The return of the hot ductility on the cooling cycle is clearly below the Laves eutectic temperature at 1125°C, which emphasises the significance of this eutectic.

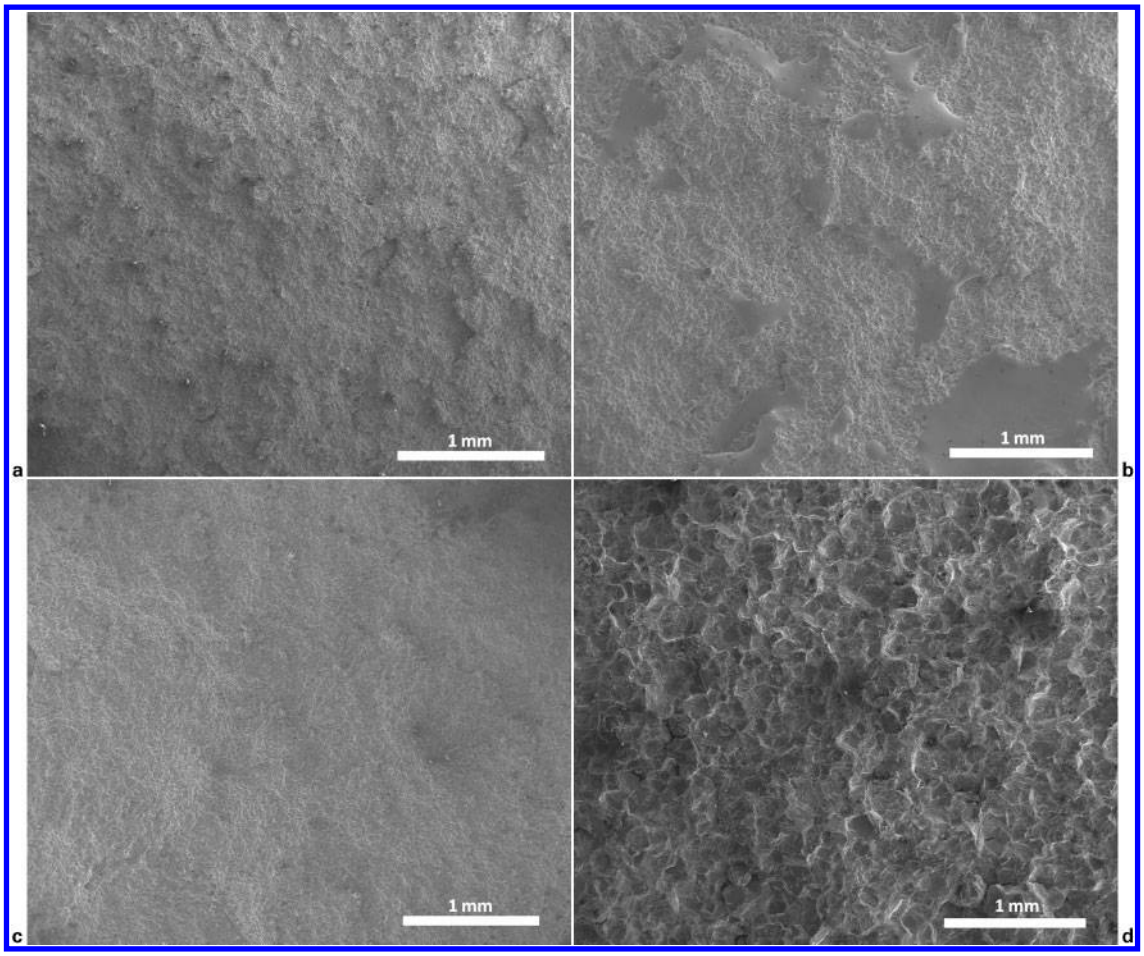

a 954°C/1 h at 1172°C; *b* 954°C/15 h at 1189°C; *c* 982°C/1 h at 1178°C; *d* 1050°C/3 h + 954°C/1 h at 1177°C

9 Images (SEM–SE) of fracture surfaces achieved at on-heating tests

The low heating and cooling rates in the DSC thermographs reflect a more equilibrium type of thermal cycle as compared with the weld thermal cycle and indicate that the peak temperature used in the Gleeble testing (1195°C) is well above the Laves eutectic reaction at 1115–1125°C, but below the NbC reaction at 1262–1286°C, as shown in Table 6. In Fig. 15, as in Fig. 14, NbC precipitates can clearly be seen being only partially dissolved by constitutional liquation which cannot account for the substantial amount of Laves eutectic agglomerates in the vicinity. It is therefore reasonable to believe that the very high Nb concentration left by the rapidly dissolved δ phase (Fig. 8) adds to the presence of such abundant Laves eutectics at the carbides. Note the limited amount of eutectics in the material without δ phase (1050°C/3 h + 954°C/1 h) in Fig. 14 and also the favourable on-heating hot ductility seen in Fig. 3.

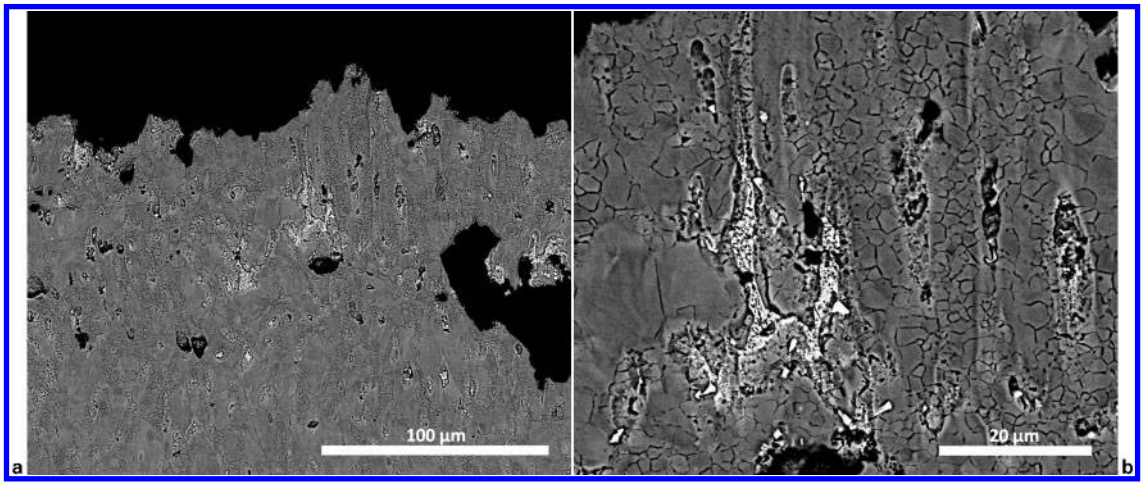

10 Eutectic liquid at *a* low and *b* high magnification in heavily deformed material close to fracture surface from on-heating test at 1077°C: material heat treated at 954°C/15 h

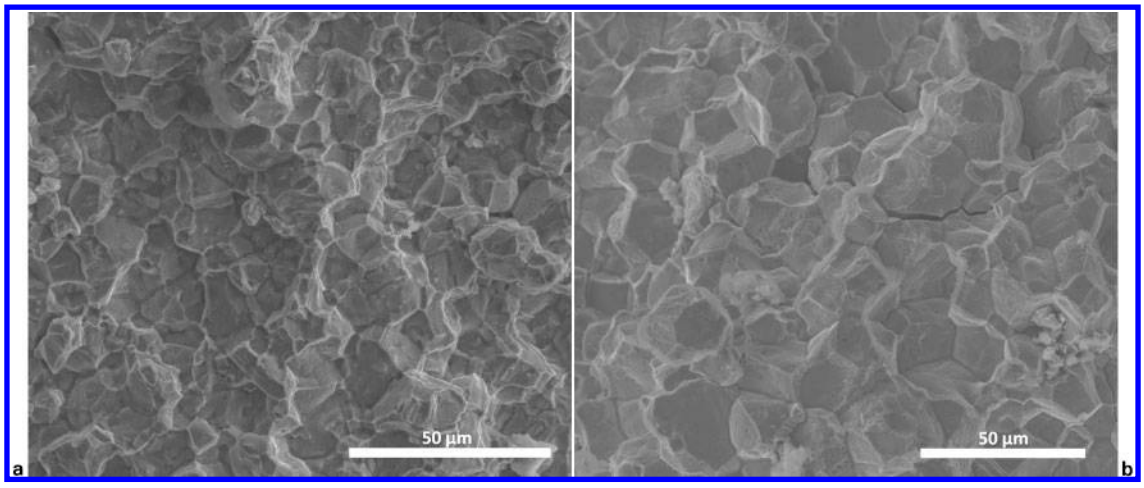

a 954°C/1 h at 1172°C; *b* 982°C/1 h at 1178°C

11 Fracture surfaces from on-heating tests

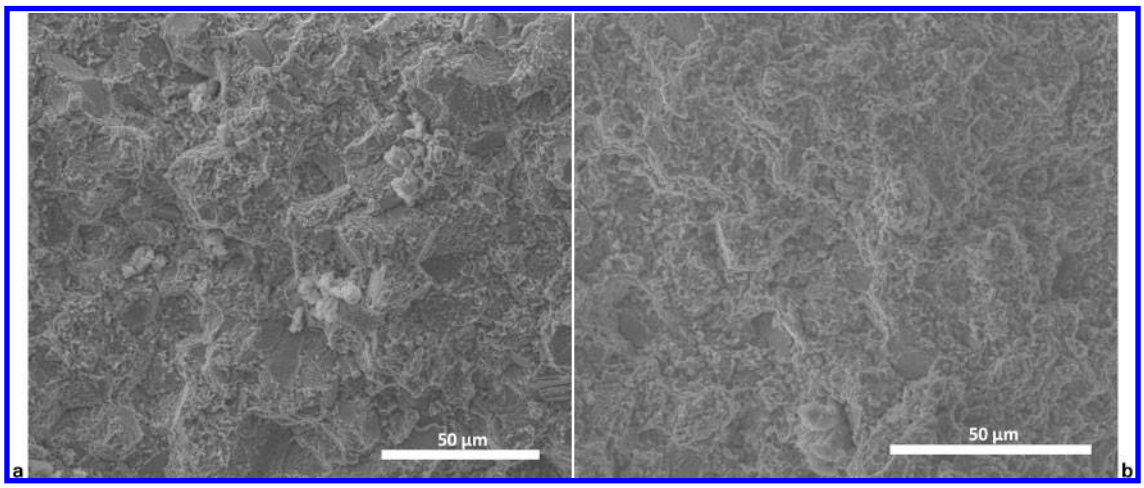

12 Fracture surfaces from on-heating testing at 1126°C on material heat treated at *a* 954°C/1 h and *b* 982°C/1 h

Combining all weldability measures in Table 3 enables the creation of an overall ranking shown in Table 7. It is interesting to see that even though the 954°C/15 h treatment provides a microstructure being the most susceptible towards liquation, it shows the best overall ranking followed by 982°C/1 h, 954°C/1 h and 1050°C/3 h + 954°C/1 h respectively.

As a measure for weldability this ranking may be partly disputed, since it does not take into account any healing mechanism, which is related to the presence of eutectics in the actual alloy.[16]

In an overall perspective, there are two striking features in the on-heating ductility curves in comparison with the on-cooling curves implicit in Fig. 3. The first feature is the strong temperature shift towards lower temperatures (DRT), which are all well below the Laves eutectic temperature. The second feature is that the ductility is not fully recovered (DRR<1).

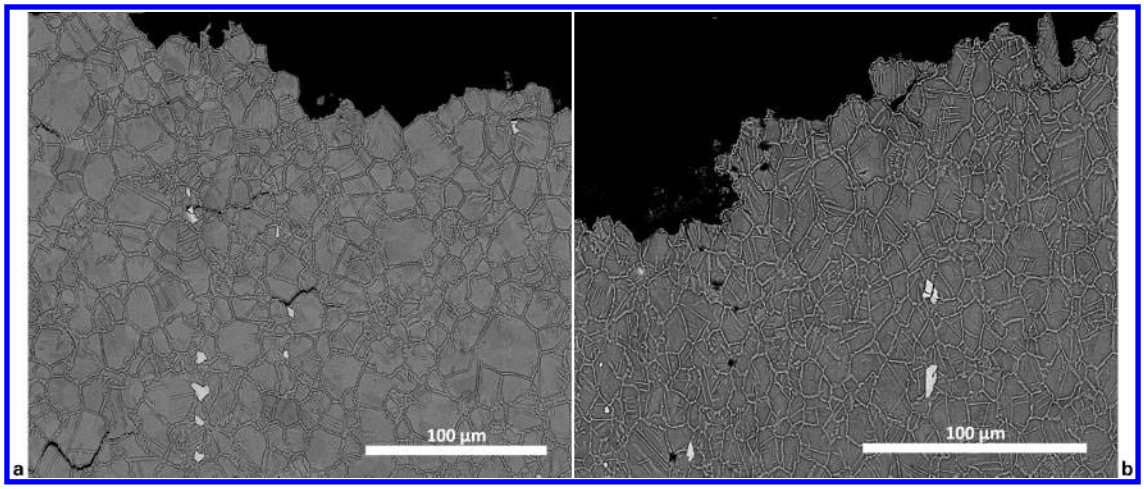

13 Images (SEM–BSE) of longitudinal cross-sections from on-heating test at 1126°C of *a* 954°C /1 h and *b* 982°C/1 h

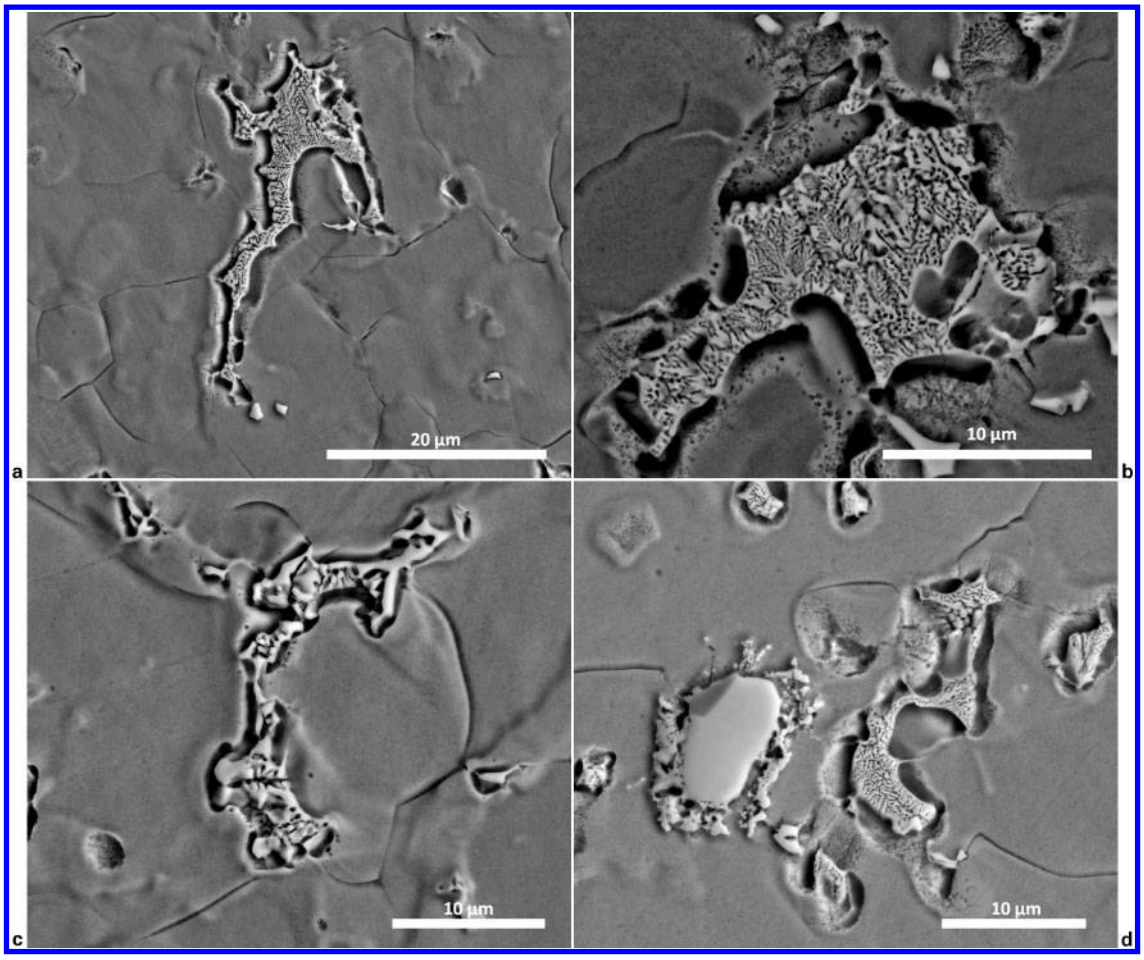

a 954°C/15 h at 1068°C; *b* 954°C/1 h at 1048°C; *c* 982°C/1 h at 1079°C; *d* 1050°C/3 h + 954°C/1 h at 1027°C

14 Images (SEM–BSE) of longitudinal cross-section revealing eutectic constituent taken from on-cooling tests: note erosion effects adjacent to eutectics due to electrolytic etching

Trace elements such as S, P and B are known to cause embrittlement in superalloys by accumulation at grain boundaries, and are accordingly kept at lowest possible level in the manufacturing.[3–5] Such elements are also known to produce low melting point eutectics due to their very low solubility in the matrix at low temperatures. Such eutectics, although in small amounts, may explain why ductility does not return before these eutectics have properly solidified. For example, S forms a eutectic with Ni that solidifies at 637°C,[17] and this may offer an explanation for the general appearance of the suppressed on-cooling ductility curves. The presence of such solidified eutectics at grain boundaries may also explain why ductility is not fully recovered (DRR<1), even when the ductility recovery process is completed.

The governing factors behind the differences observed in the ductility behaviour in the present study must accordingly be associated with the expected tendencies

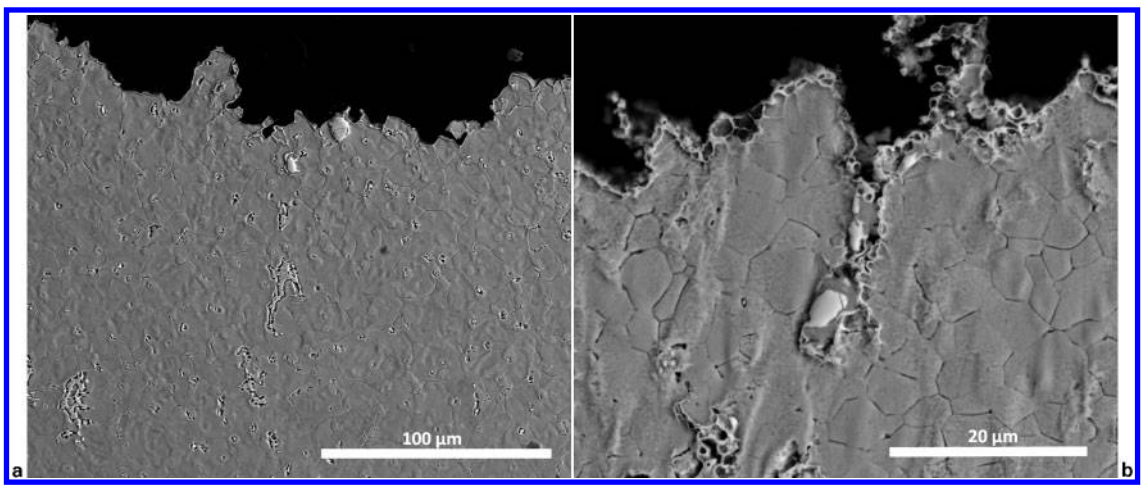

a 954°C/15 h at 1068°C; *b* 982°C/1 h at 950°C

15 Images (SEM–BSE) of longitudinal cross-section from on-cooling test disclosing unharmed NbC at top of specimens

Table 7 Ranking based on estimated Gleeble welding parameters in Table 3

Treatments	NDT	BTR	DRR	RDR	Score	Ranking
954°C/1 h	2	2	4	3	11	3
982°C/1 h	3	3	2	2	10	2
954°C/15 h	4	1	1	1	7	1
1050°C/3 h+954°C/1 h	1	4	3	4	12	4

to accumulate such deleterious trace elements at the grain boundaries during the overheating cycle imposed in the Gleeble testing performed. For example, it is well known that a material with larger grains possesses inferior weldability in terms of cracking than the same material in a smaller grain condition. One reasonable explanation is that for a given amount of trace elements a larger portion of the grain boundary interface area will be covered in a large grain size material in comparison with a small grain material producing a more intensive eutectic reaction at the boundaries.

It is clear that the grain size depends not only on the actual heat treatments prior to Gleeble testing but also on the temperature exposure during the actual testing, as is evident from the on-cooling grain size numbers in Table 5. The role of δ phase in the control of grain size due to its pinning effect in the manufacturing of Alloy 718 is well know, but it may also exhibit control by the same mechanism during the very fast heating in the Gleeble testing. Thus, the material with the largest amount of δ phase (the one heat treated at 954°C for 15 h) with an grain size of ASTM 11 before Gleeble testing is the material that exhibits the smallest on-cooling grain size (ASTM 10). The material without any δ phase (the one heat treated at 1050°C for 3 h) had a grain size of ASTM 2 after heat treatment and significantly larger grains (ASTM 3) when exposed to the testing thermal cycle compared to the other conditions. The reason why the measured grain size is reduced from ASTM 2 to 3 during testing may be associated with small differences in grain size among the samples measured. The materials of the other two heat treatments with intermediate amounts of δ phase have both a fine grain size of ASTM 8. Here, the grain size before testing was ASTM 9 (954°C/1 h) and 11 (982°C/1 h). Thus, the presence of δ phase may be the governing factor for the hot ductility response during welding (and hot cracking) by the beneficial influence on the grain size control to limit accumulation of deleterious trace elements.

Conclusions

Constitutional liquation of NbC phase is found to be assisted by δ phase, which limits the hot ductility of Alloy 718. Based on Gleeble testing, it is indicated that a coarse grain material (ASTM 3) forecasts limited weldability, whereas a material containing large amounts of δ phase forecasts improved weldability. The δ phase is believed to be beneficial in grain boundary pinning when significantly present, thus limiting the grain growth and consequently also reducing the trace elements at grain boundaries at very high temperatures.

Acknowledgements

At the Department of Mechanical and Industrial Engineering at the University of Manitoba we sincerely acknowledge Dr O. A. Ojo for all fruitful comments and advice, Dr Krutika Vishwakarma and Mr Mike Boskwick for all help with the Gleeble testing and Christopher Knee at the Department of inorganic chemistry at Göteborg University for performing the DSC measurements.

References

1. R. Vincent: 'Precipitation around welds in the nickel-base superalloy, INCONEL 718', *Acta Metall.*, 1985, **33**, 1205–1216.
2. G. Sjöberg, J. Andersson and A. Sjunnesson: 'New materials in the design and manufacturing of hot structures for aircraft engines – Allvac 718Plus', Proc. 19th Int. Symp. on 'Air breathing engines', Montreal, Canada, September 2009, International Association of Airbreathing Engines, Paper 1286.
3. W. R. Sun, S. R. Guo, D. Z. Lu and Z. O. Hu: 'Effect of sulfur on the solidification and segregation in Inconel 718 alloy', *Mater. Lett.*, 1997, **31**, 195–200.
4. S. Benhadad, N. L. Richards and M. C. Chaturvedi: 'The influence of minor elements on the weldability of an INCONEL 718-type superalloy', *Metall. Mater. Trans. A*, 2002, **33A**, 2005–2017.
5. S. Benhadad, N. L. Richards, U. Prasad, H. Guo and M. C. Chaturvedi: in 'Superalloys 2000', (ed. T. M. Pollock *et al.*), 703–711; 2000, Warrendale, PA, TMS.
6. C. D. Lundin: 'Historical development of the high speed time–temperature controller for welding research, The Gleeble', Proc. 7th Annu.ISPS Conf., Tskukuba, Japan, Dynamic Systems International and International Symposium on Physical Simulation, January 1997, 283–289.
7. J. C. Lippold, S. D. Kiser and J. N. DuPont: 'Welding metallurgy and weldability of nickel-base superalloys'; 2009, Hoboken, NJ, John Wiley and Sons.
8. C. D. Lundin, C. Y. P. Qiao, T. P. S. Gill and G. M. Goodwin: 'Hot ductility and hot cracking behavior of modified 316 stainless steels designed for high-temperature service', *Weld. J.*, May 1993, 189–200.
9. H. Guo, M. C. Chaturvedi and N. L. Richards: 'Effect of boron concentration and grain size on weld heat affected zone microfissuring in Inconel 718 base superalloys', *Sci. Technol. Weld. Join.*, 1999, **4**, 257–264.
10. Y. M. Yaman and M. C. Kushan: 'Hot cracking susceptibilities in the heat-affected zone of electron-beam welded inconel 718', *J. Mater. Sci. Lett.*, 1998, **17**, 1231–1234.
11. M. E. Mehl and J. C. Lippold: in 'Superalloys 718, 625, 706 and various derivatives', (ed. E. A. Loria), 731–741; 1997, Warrendale, PA, TMS.
12. H. R. Zhang and O. A. Ojo: 'Non-equilibrium liquid phase dissolution of δ phase precipitates in a nickel-based superalloy', *Philos. Mag. Lett.*, 2009, **89**, 787–794.
13. L. Qiang: 'HAZ microstructural evolution in Alloy 718 after multiple repair and PWHT cycles', PhD thesis, The Ohio State University, Columbus, OH, USA, 1999.
14. M. Qian: 'An Investigation of The Repair Weldability of Waspaloy and Alloy 718', PhD thesis, The Ohio State University, Columbus, USA, 2002.
15. B. Radhakrishnan and R. G. Thompson: 'A phase diagram approach to study liquation cracking in alloy 718', *Metallurgical Transactions A*, 1991, **22A**, 887-902.
16. J. Andersson, G. Sjöberg and H. Hänninen: in 'Hot Cracking Phenomena in Welds III', (ed. J.C. Lippold, T.H. Boellinghaus, and C.E. Cross), 415-428; 2011, Columbus, OH, Springer Verlag.
17. C. Loier and J. Y. Boos: 'Striation and Faceting of Grain Boundaries in Nickel Due to Sulfur and Other Elements', *Metallurgical Transactions A*, 1981, **12A**, 129-135.